Annex 8

Hydrodynamic Theory of Drop Detachment from Micro-Pores with Application to Membrane Emulsification

Krassimir D. Danov, Nikolai C. Christov, Darina K. Danova, and Peter A. Kralchevsky

Laboratory of Chemical Physics and Engineering, Faculty of Chemistry, University of Sofia, 1 J. Bourchier Ave., 1164 Sofia, Bulgaria

Abstract. Here, we investigate theoretically the production of monodisperse emulsions with the help of microporous membranes. To understand the mechanism of drop detachment from a pore, theoretical calculations for the case without cross flow have been performed. The Navier-Stokes equation has been solved and the fields of velocity and pressure have been computed for the interior and exterior of oil drop, which is growing at the orifice of a pore. The driving force of the drop detachment turns out to be the viscous stress due to the flow of the liquid, supplied by the pore, which feeds the growing drop. For drop detachment, it is not necessary the viscous stress to cause a violation of the force balance in the system. Instead, it is sufficient the viscous stress to produce a deformation in the drop shape, which leads to the appearance of a necking instability, in analogy with the case of a pendant drop. This instability brings about the drop detachment, which corresponds to a transition from stable to unstable equilibrium. The driving force, due to the liquid flow inside the growing drop, and the resistance force, due to the outer fluid, are quantified.

1. Introduction

The method of membrane emulsification has found a considerable development and many applications during the last decade. The method has been applied in many fields, in which monodisperse emulsions are needed. An example is the application in food industry for production of oil-in-water (O/W) emulsions: dressings, artificial milk, cream liqueurs, as well as for preparation of some water-in-oil (W/O) emulsions: margarine and low-fat spreads. Another application of this method is for fabrication of monodisperse colloidal particles: silica-hydrogel and polymer microspheres; porous and cross-linked polymer particles; microspheres containing carbon black for toners, etc. A third field of utilization is for

obtaining multiple emulsions and microcapsules, which have found applications in pharmacy and chemotherapy. Closely related to the membrane emulsification is the method employing capillary tubes and micro-channels to produce monodisperse emulsions.

A key problem of membrane emulsification is to explain and predict the dependence of the drop diameter, d_{drop}, on the experimental parameters: pore diameter, d_{pore}, applied cross flow in the continuous phase, flux of the disperse phase along the pores, viscosity of the oil and water phases, interfacial tension and kinetics of surfactant adsorption, etc. (Here and hereafter we call "disperse" the phase from which the drops are made, despite the fact that this phase is continuous before the drop detachment from the membrane.) The values of the ratio d_{drop}/d_{pore}, reported in different experimental works, vary in the range from 2 to 10; the reasons for this variation have not yet been well understood. Below we briefly consider the major factors affecting the ratio d_{drop}/d_{pore}.

The *flow of the disperse phase* along the pores of the emulsification membrane can be varied by controlling the pressure difference applied across the membrane. The experiments show that typically an increase of the transmembrane flow (or of the applied pressure) results in a greater mean drop size and in a higher polydispersity of the formed drops. Moreover, one can distinguish two regimes of transmembrane flow: (i) fixed flow rate and (ii) fixed pressure. The former regime takes place in the emulsification setups using a bunch of capillaries or micro-channels, where the disperse phase is usually supplied by a pump. The second regime is typical for the standard emulsification setups, in which the disperse phase is pushed across the membrane by nitrogen gas from a bottle. In this case the gas plays the role of a buffer which keeps constant the applied pressure difference across the membrane; on the other hand, the flow rate along a given pore may oscillate when drops grow and detach at its orifice.

The oil-water *interfacial tension*, σ, is recognized to be the major retention force, that is the force which keeps the drops attached to the membrane surface. Greater σ is expected to cause the production of larger emulsion drops. Complications arise from the fact that, as a rule, a surfactant (emulsifier) is dissolved in the continuous phase to stabilize the produced emulsion against drop coalescence. Since the surfactant has a finite rate of adsorption at the oil water interface, the coverage of the drop surface with adsorbed surfactant molecules decreases (and the dynamic value of σ increases) when the frequency of drop release from the pores grows. The latter effect could explain, at least in part, the aforementioned rise in the drop size with the increase of the transmembrane pressure.

Our study is aimed at revealing the hydrodynamic factors that govern the drop detachment from the orifice of a pore. For this goal, we solve the hydrodynamic problem in the three spatial regions: (i) inside the pore; (ii) inside the growing drop; and (iii) in the outer liquid phase. The driving force, due to the liquid flow inside the growing drop, and the resistance force, due to the outer fluid, are quantified. Our working hypothesis is that these forces cause deformation of the drop surface that leads to a necking instability and drop detachment, as it is with the pendant drops.

2. Kinematics of drop expansion

We consider the expansion of an emulsion drop, which is growing at the tip of a capillary. Our purpose is to model the formation of drops at the openings of the pores of an emulsification membrane. We are dealing with microscopic drops, for which the gravitational deformation of the drop shape is negligible. Here, we consider the simpler case, in which there is no cross-flow in the outer liquid phase; i.e. the only motion in the outer fluid is caused by the drop formation.

Because we are dealing with small drops, we will simplify our treatment by the assumption that the drop surface is (approximately) spherical. The membrane pore will be modeled as a cylindrical channel, see Fig. 1. The radius of the drop surface will be denoted by R_s, while the inner radius of the channel (pore) – by R_p. To describe the process of drop formation, we will use cylindrical coordinates (r,z), where the z-axis coincides with the axis of rotational symmetry of the system, and the plane $z = 0$ coincides with the outer membrane surface (Fig. 1).

The inner and outer liquids will be referred as "phase a" and "phase b", respectively. For example, "phase a" could be oil and "phase b" – water, or vice versa. Due to the symmetry, the velocity field in the respective phase can be expressed in the form:

$$\mathbf{v}_a = u_a \mathbf{e}_r + w_a \mathbf{e}_z , \quad \mathbf{v}_b = u_b \mathbf{e}_r + w_b \mathbf{e}_z \tag{2.1}$$

where $\mathbf{e}_r$ and $\mathbf{e}_z$ are the unit vectors of the respective axes. Inside the channel, far from its orifice, we have Poiseuille flow of the inner liquid:

$$u_a = 0 , \quad w_a = 2 v_m \left(1 - \frac{r^2}{R_p^2}\right) \quad \text{for } 0 \le r \le R_p \quad \text{and} \quad z \to -\infty \tag{2.2}$$

Here v_m is the mean velocity, and the subscript "a" denotes the inner liquid phase. The flow rate, Q, of the inner liquid is:

$$Q = \pi R_{\mathrm{p}}^2 v_{\mathrm{m}} = \frac{\mathrm{d}V}{\mathrm{d}t} \tag{2.3}$$

where V is the volume of the growing drop and t is time. The volume, V, can be expressed in the form:

$$V = \frac{\pi R_{\mathrm{p}}^3}{3} \frac{2+\cos\alpha}{(1+\cos\alpha)^2} \sin\alpha \tag{2.4}$$

where the angle α is shown in Fig. 1. The differentiation of Eq. (2.4), in view of Eq. (2.3), yields:

$$\frac{\mathrm{d}\alpha}{\mathrm{d}t} = \frac{v_{\mathrm{m}}}{R_{\mathrm{p}}} (1+\cos\alpha)^2 \tag{2.5}$$

The time derivative of the drop radius is:

$$\frac{\mathrm{d}R_{\mathrm{s}}}{\mathrm{d}t} = \frac{\mathrm{d}}{\mathrm{d}t}\left(\frac{R_{\mathrm{p}}}{\sin\alpha}\right) = -v_{\mathrm{m}} \frac{1+\cos\alpha}{1-\cos\alpha} \cos\alpha \tag{2.6}$$

Likewise, for the z-coordinate of the drop center, z_{d}, we obtain:

$$\frac{\mathrm{d}z_{\mathrm{d}}}{\mathrm{d}t} = -\frac{\mathrm{d}}{\mathrm{d}t}(R_{\mathrm{p}} \cot\alpha) = v_{\mathrm{m}} \frac{1+\cos\alpha}{1-\cos\alpha} \tag{2.7}$$

We will assume that the relative motion of the material points on the drop surface corresponds to an isotropic surface expansion. Physically, this corresponds to the case when adsorbed surfactant molecules are present at the interface, and the latter behaves as an elastic membrane owing to the considerable surface (Gibbs) elasticity. For isotropic interfacial expansion, we have $\theta/\alpha = s$ = constant, where θ is the polar coordinate of a given surface material point (Fig. 1). Let us denote by $(r_{\mathrm{s}},z_{\mathrm{s}})$ the coordinates of a material point on the drop surface with respect to the immobile cylindrical coordinate system bound to the channel of the pore (Fig. 1). Then, we obtain:

$$r_{\mathrm{s}} = R_{\mathrm{s}} \sin(s\alpha), \quad z_{\mathrm{s}} = z_{\mathrm{d}} + R_{\mathrm{s}} \cos(s\alpha) \tag{2.8}$$

The differentiation of Eq. (2.8) at fixed s, along with Eqs. (2.5)–(2.7), yields the radial and axial resultants of the surface velocity:

$$u_{\mathrm{s}} = \frac{\mathrm{d}r_{\mathrm{s}}}{\mathrm{d}t} = v_{\mathrm{m}} \frac{1+\cos\alpha}{1-\cos\alpha} (s\cos\theta\sin\alpha - \sin\theta\cos\alpha) \tag{2.9}$$

$$w_{\mathrm{s}} = \frac{\mathrm{d}z_{\mathrm{s}}}{\mathrm{d}t} = v_{\mathrm{m}} \frac{1+\cos\alpha}{1-\cos\alpha} (1 - s\sin\theta\sin\alpha - \cos\theta\cos\alpha) \tag{2.10}$$

Further, with the help of Eqs. (2.9) and (2.10), and the relationship

$$\mathbf{v}_{\mathrm{s}} = u_{\mathrm{s}}\mathbf{e}_r + w_{\mathrm{s}}\mathbf{e}_z \tag{2.11}$$

we deduce expressions for the normal and tangential projections of the surface velocity with respect to the drop surface:

$$\mathbf{n}\cdot\mathbf{v}_{\mathrm{s}} = v_{\mathrm{m}}\frac{1+\cos\alpha}{1-\cos\alpha}(\cos\theta-\cos\alpha) \tag{2.12}$$

$$\mathbf{t}\cdot\mathbf{v}_{\mathrm{s}} = v_{\mathrm{m}}\frac{1+\cos\alpha}{1-\cos\alpha}(s\sin\alpha-\sin\theta) \tag{2.13}$$

where **n** and **t** are the running unit normal and tangent to the drop surface (Fig. 1):

$$\mathbf{n} = \mathbf{e}_r\sin\theta + \mathbf{e}_z\cos\theta\,, \quad \mathbf{t} = \mathbf{e}_r\cos\theta - \mathbf{e}_z\sin\theta \tag{2.14}$$

3. Basic hydrodynamic equations

During membrane emulsification, the typical process of drop detachment occurs at small values of the Reynolds number. To check that, we present Eq. (2.3) in the form:

$$\pi R_{\mathrm{p}}^2 v_{\mathrm{m}} \approx \frac{4}{3}\pi R_{\mathrm{d}}^3/\Delta t \tag{3.1}$$

where Δt is the period of drop formation and R_{d} is the radius of the detached drops. Then, the Reynolds number could be estimated as:

$$\mathrm{Re} = \frac{\rho v_{\mathrm{m}} R_{\mathrm{p}}}{\eta} \approx \frac{4\rho R_{\mathrm{d}}^3}{3\eta R_{\mathrm{p}}\Delta t} \tag{3.2}$$

Substituting typical parameter values: density ρ = 1 g/cm^3; dynamic viscosity η = 0.01 poises, Δt = 0.1 s; $R_{\mathrm{d}} \approx 3R_{\mathrm{p}}$, and $R_{\mathrm{p}} \le 20$ μm, from Eq. (3.2) we obtain Re ≈ 0.14. Hence, the Reynolds number is small and the classical Stokes equations can be used to describe the flow in the inner and outer liquid phases:

$$\nabla\cdot\mathbf{v}_{\mathrm{a}} = 0\,, \quad \nabla p_{\mathrm{a}} = \eta_{\mathrm{a}}\nabla^2\mathbf{v}_{\mathrm{a}} \tag{3.3}$$

$$\nabla\cdot\mathbf{v}_{\mathrm{b}} = 0\,, \quad \nabla p_{\mathrm{b}} = \eta_{\mathrm{b}}\nabla^2\mathbf{v}_{\mathrm{b}} \tag{3.4}$$

where ∇ is the spatial gradient operator; as usual p, **v**, and η stand for pressure, velocity, and dynamic viscosity; the subscripts "a" and "b" denote quantities related to the inner and outer liquid phases, respectively. It is convenient to introduce dimensionless variables, denoted by tilde, as follows:

$$r \equiv R_{\mathrm{p}}\tilde{r}\,, \quad z \equiv R_{\mathrm{p}}\tilde{z}\,, \quad \mathbf{v}_{\mathrm{a}} \equiv v_{\mathrm{m}}\tilde{\mathbf{v}}_{\mathrm{a}}\,, \quad \mathbf{v}_{\mathrm{b}} \equiv v_{\mathrm{m}}\tilde{\mathbf{v}}_{\mathrm{b}} \tag{3.5}$$

$$p_{\mathrm{a}} \equiv p_\infty + \frac{2\sigma}{R_{\mathrm{s}}} + \frac{\eta_{\mathrm{a}} v_{\mathrm{m}}}{R_{\mathrm{p}}}\tilde{p}_{\mathrm{a}}\,, \quad p_{\mathrm{b}} \equiv p_\infty + \frac{\eta_{\mathrm{b}} v_{\mathrm{m}}}{R_{\mathrm{p}}}\tilde{p}_{\mathrm{b}} \tag{3.6}$$

where p_∞ is the equilibrium bulk pressure in the outer phase far from the forming drop; σ is the oil/water interfacial tension. With the help of Eqs. (2.1), (3.5) and (3.6), we bring Eqs. (3.3) and (3.4) in the form:

$$\frac{1}{\tilde{r}}\frac{\partial}{\partial \tilde{r}}(\tilde{r}\,\tilde{u}_{\rm f}) + \frac{\partial \tilde{w}_{\rm f}}{\partial \tilde{z}} = 0 \tag{3.7}$$

$$\frac{\partial}{\partial \tilde{r}}\left[\frac{1}{\tilde{r}}\frac{\partial}{\partial \tilde{r}}(\tilde{r}\,\tilde{u}_{\rm f})\right] + \frac{\partial^2 \tilde{u}_{\rm f}}{\partial \tilde{z}^2} = \frac{\partial \tilde{p}_{\rm f}}{\partial \tilde{r}} \tag{3.8}$$

$$\frac{1}{\tilde{r}}\frac{\partial}{\partial \tilde{r}}\left(\tilde{r}\frac{\partial \tilde{w}_{\rm f}}{\partial \tilde{r}}\right) + \frac{\partial^2 \tilde{w}_{\rm f}}{\partial \tilde{z}^2} = \frac{\partial \tilde{p}_{\rm f}}{\partial \tilde{z}} \tag{3.9}$$

where f = a, b. Equations (3.7)–(3.9), along with the respective boundary conditions (see below) form a system of equations for determining $\tilde{p}_{\rm f}$, $\tilde{u}_{\rm f} = u_{\rm f}/v_{\rm m}$, and $\tilde{w}_{\rm f} = w_{\rm f}/v_{\rm m}$. To obtain separate equations for the separate unknown variables, we will use a standard hydrodynamic approach, viz. we will introduce the dimensionless stream function, $\psi_{\rm f}$, and vorticity function, $\omega_{\rm f}$, as follows:

$$\tilde{u}_{\rm f} \equiv \frac{\partial \psi_{\rm f}}{\partial \tilde{z}}, \quad \tilde{w}_{\rm f} \equiv -\frac{1}{\tilde{r}}\frac{\partial}{\partial \tilde{r}}(\tilde{r}\,\psi_{\rm f}) \tag{3.10}$$

$$\omega_{\rm f} \equiv \frac{\partial \tilde{u}_{\rm f}}{\partial \tilde{z}} - \frac{\partial \tilde{w}_{\rm f}}{\partial \tilde{r}} \qquad ({\rm f} = {\rm a, b}) \tag{3.11}$$

In view of Eq. (3.10), the continuity equation, Eq. (3.7), is automatically satisfied. In addition, from Eqs (3.8) and (3.9) we obtain:

$$L[\psi_{\rm f}] = \omega_{\rm f}, \quad L[\omega_{\rm f}] = 0 \qquad ({\rm f} = {\rm a, b}) \tag{3.12}$$

where the linear operator, L, is defined as

$$L[f] \equiv \frac{\partial}{\partial \tilde{r}}\left[\frac{1}{\tilde{r}}\frac{\partial}{\partial \tilde{r}}(\tilde{r}\,f)\right] + \frac{\partial^2 f}{\partial \tilde{z}^2} \tag{3.13}$$

The pressure $\tilde{p}_{\rm f}$ is related to the vorticity, $\omega_{\rm f}$. To derive this relationship, we first substitute $\partial \tilde{w}_{\rm f}/\partial \tilde{z}$ from Eq. (3.7) into Eq. (3.9), and next, we apply the definition of $\omega_{\rm f}$ in Eq. (3.11):

$$\frac{\partial \tilde{p}_{\rm f}}{\partial \tilde{z}} = -\frac{1}{\tilde{r}}\frac{\partial}{\partial \tilde{r}}(\tilde{r}\,\omega_{\rm f}) \qquad ({\rm f} = {\rm a, b}) \tag{3.14}$$

4. Boundary conditions

An important step in the modeling of the drop expansion is to transform the hydrodynamic boundary conditions in the terms of stream and vorticity functions.

(a) At the axis of symmetry, $\tilde{r} = 0$, the radial velocity, u_f, and the curl of the fluid flow must be zero, irrespective of the value of z. Then, from Eqs. (3.10) and (3.11) one obtains:

$$\psi_f = \omega_f = 0 \quad \text{at } \tilde{r} = 0 \quad (f = a, b) \tag{4.1}$$

(b) Inside the channel of the pore, far from its orifice, we have Poiseuille flow with a parabolic velocity profile given by Eq. (2.2). Then, from Eqs. (2.2), (3.10) and (3.11) we derive:

$$\psi_a = -\tilde{r} + \frac{\tilde{r}^3}{2}, \quad \omega_a = 4\tilde{r} \quad \text{at } 0 \le \tilde{r} \le 1 \text{ and } \tilde{z} \to -\infty \tag{4.2}$$

(c) Next, at the solid wall of the cylindrical pore channel ($\tilde{r} = 1$, see Fig. 1) we must have $u_a = w_a = 0$. Substituting $\tilde{r} = 1$ in Eq. (4.2) we get $\psi_a = -1/2$. Further, we substitute the latter results in the expression for $\tilde{w}_f$ in Eq. (3.10) to derive:

$$\psi_a = -\frac{1}{2}, \quad \frac{\partial \psi_a}{\partial \tilde{r}} = \frac{1}{2} \quad \text{for } \tilde{r} = 1 \text{ and } \tilde{z} \le 0 \tag{4.3}$$

Likewise, we have $u_b = w_b = 0$ at the solid surface $\tilde{z} = 0$ for $\tilde{r} \ge 1$, which represents the boundary of the membrane with the outer fluid (Fig. 1). For this boundary, we obtain:

$$\psi_b = -\frac{1}{2\tilde{r}}, \quad \frac{\partial \psi_b}{\partial \tilde{z}} = 0 \quad \text{at } \tilde{r} \ge 1 \text{ and } \tilde{z} = 0 \tag{4.4}$$

Here we have used the fact that the substitution of $\psi_b \propto 1/\tilde{r}$ into Eq. (3.10) yields $\tilde{w}_f = 0$; the constant of proportionality is determined from the condition $\psi_b = \psi_a = -1/2$ at $\tilde{r} = 1$, see Eq. (4.3).

(d) At the drop surface we impose the kinematic boundary condition $\mathbf{n} \cdot \mathbf{v}_a = \mathbf{n} \cdot \mathbf{v}_b = \mathbf{n} \cdot \mathbf{v}_s$, where $\mathbf{n} \cdot \mathbf{v}_s$ is given by Eq. (2.12). From these relationships, we derive (Appendix A):

$$\psi_a = \psi_b = -\frac{1}{2}\left(1 - \frac{2\cos\alpha}{1+\cos\theta}\right)\frac{1+\cos\alpha}{1-\cos\alpha}\frac{\sin\theta}{\sin\alpha} \quad \text{(at drop surface)} \tag{4.5}$$

As discussed after Eq. (2.7), here we treat the expanding drop surface as an expanding elastic membrane. In this case, we should have also equal tangential components of the velocities at the interface: $\mathbf{t} \cdot \mathbf{v}_a = \mathbf{t} \cdot \mathbf{v}_b = \mathbf{t} \cdot \mathbf{v}_s$ (no slip boundary condition), where $\mathbf{t} \cdot \mathbf{v}_s$ is given by Eq. (2.13). From these equations the following boundary condition of the Neumann type for the stream function is derived (Appendix A):

$$\frac{\partial \psi_f}{\partial n} + \psi_f \sin\alpha = \frac{1+\cos\alpha}{1-\cos\alpha}(s\sin\alpha - \sin\theta) \quad \text{(at drop surface)} \tag{4.6}$$

where f = a, b. The directional derivative is:

$$\frac{\partial \psi_{\rm f}}{\partial n} = \mathbf{n}\cdot\nabla\psi_{\rm f} = \sin\theta\frac{\partial \psi_{\rm f}}{\partial \tilde{r}} + \cos\theta\frac{\partial \psi_{\rm f}}{\partial \tilde{z}} \tag{4.7}$$

In view of Eqs. (4.5) and (4.6), the problem is split to two separate boundary problems in phases "a" and "b".

5. Hydrodynamic force acting on the emulsion drop

5.1. Integral expressions

The hydrodynamic force, F, acting on the drop surface, *S*, is a difference of contributions from phases "a" and "b", $\mathbf{F}_{\rm a}$ and $\mathbf{F}_{\rm b}$, respectively:

$$\mathbf{F}_{\rm a} = \int_S {\rm d}s\,\mathbf{n}\cdot\mathbf{P}_{\rm a}\,, \quad \mathbf{F}_{\rm b} = -\int_S {\rm d}s\,\mathbf{n}\cdot\mathbf{P}_{\rm b} \tag{5.1}$$

where $\mathbf{n}$ is an outer normal to the drop surface. In Eq. (5.1), the pressure tensors, $\mathbf{P}_{\rm a}$ and $\mathbf{P}_{\rm b}$, obey the Newton's law for a viscous fluid:

$$\mathbf{P}_{\rm f} \equiv p_{\rm f}\mathbf{U} - \eta_{\rm f}[\nabla\mathbf{v}_{\rm f} + (\nabla\mathbf{v}_{\rm f})^{\rm tr}] \qquad ({\rm f} = {\rm a}, {\rm b}) \tag{5.2}$$

where $\mathbf{U}$ is the spatial unit tensor and the superscript "tr" means transposition. The Stokes equations, Eqs. (3.3) and (3.4), are equivalent to $\nabla\cdot\mathbf{P}_{\rm f} = 0$. Then, in accordance with the Gauss-Ostrogradsky theorem, the forces given by Eq. (5.1) can be calculated at every mathematical surface that together with *S* forms a closed surface (Faxen theorem). The calculations are simpler if we choose the surface $z = 0$ as integration domain for both forces in Eq. (5.1):

$$\mathbf{F}_{\rm a} = 2\pi\mathbf{e}_z\int_0^{R_{\rm p}} {\rm d}r\, r\left(P_{{\rm a},zz} - p_\infty - \frac{2\sigma}{R_{\rm s}}\right) \tag{5.3}$$

$$\mathbf{F}_{\rm b} = 2\pi\mathbf{e}_z\int_{R_{\rm p}}^{\infty} {\rm d}r\, r\,(P_{{\rm b},zz} - p_\infty) \tag{5.4}$$

where the values of the tensorial components $P_{{\rm a},zz}$ and $P_{{\rm b},zz}$ are taken at $z = 0$. The integration in Eq. (5.3) is over the cross-section of the pore at its orifice (Fig. 1), while the integration in Eq. (5.4) is over the flat solid surface that encircles the pore orifice. In Eqs. (5.3) and (5.4), we have subtracted the static pressure in the respective phase from the pressure tensor. Thus, $\mathbf{F}_{\rm a}$ and $\mathbf{F}_{\rm b}$ acquire purely hydrodynamic character, and we could seek expressions for the magnitudes of these forces in the form:

$$F_{\rm a} = f_{\rm a}\eta_{\rm a}R_{\rm p}v_{\rm m}\,, \quad F_{\rm b} = f_{\rm b}\eta_{\rm b}R_{\rm p}v_{\rm m} \tag{5.5}$$

In Eq. (5.5), F_a and F_b are expressed in the known Stokes form, however the coefficients, f_a and f_b, are, in general, different from 6π.

Our goal will be to derive expressions and to obtain numerical results for the friction coefficients f_a and f_b. For this goal, we express $P_{f,zz}$ from Eq. (5.2), and use the continuity equation (3.7):

$$P_{f,zz} = p_f - 2\eta_f \frac{\partial w_f}{\partial z} = p_f + 2\eta_f \frac{1}{r}\frac{\partial}{\partial r}(r u_f) \tag{5.6}$$

where (f = a, b). The radial component of the velocity at the solid surface is zero; hence, we have $u_a(r{=}R_p) = u_b(r{=}R_p) = u_b(r{\to}\infty) = 0$. Therefore, when substituting Eq. (5.6) into Eqs. (5.3)–(5.4), and integrating, the last term in Eq. (5.6) gives zero contribution, and the result reads:

$$F_a = 2\pi \int_0^{R_p} (p_a - p_\infty - \frac{2\sigma}{R_s}) r \, dr \qquad (z = 0) \tag{5.7}$$

$$F_b = 2\pi \int_{R_p}^{\infty} (p_b - p_\infty) r \, dr \qquad (z = 0) \tag{5.8}$$

Finally, in Eqs. (5.7)–(5.8) we introduce dimensionless variables in accordance with Eqs. (3.5) and (3.6). As a result, we obtain Eq. (5.5), where the dimensionless coefficients of the hydrodynamic force are given by the expressions:

$$f_a = 2\pi \int_0^1 \widetilde{p}_a \widetilde{r} \, d\widetilde{r}\,, \quad f_b = 2\pi \int_1^{\infty} \widetilde{p}_b \widetilde{r} \, d\widetilde{r} \tag{5.9}$$

In Eq. (5.9), $\widetilde{p}_a$ and $\widetilde{p}_b$ must be estimated at $z = 0$.

To determine the pressures p_a and p_b in the phases 'a' and 'b', we need two boundary conditions. In the region 'b' this is the condition $p_b \to p_\infty$ in the bulk of phase b. To obtain the respective boundary condition in the phase 'a', we will use the Laplace equation of capillarity. For this goal, we present p_a and p_b in the form:

$$p_a \equiv p_\infty + \frac{2\sigma}{R_s} + p_{a,dyn}\,, \quad p_b \equiv p_\infty + p_{b,dyn} \tag{5.10}$$

where $p_{a,dyn}$ and $p_{b,dyn}$ are the respective dynamic contributions to the pressure. As a boundary condition, we will consider the force balance at the apex of the drop surface (Fig. 1), that is the point where the z-axis pierces the drop surface:

$$\frac{2\sigma}{R_s} + \left(p_b - 2\eta_b \frac{\partial w_b}{\partial z} \right)_{ap} = \left(p_a - 2\eta_a \frac{\partial w_a}{\partial z} \right)_{ap} \tag{5.11}$$

Substituting p_a and p_b from Eq. (5.10) into Eq. (5.11), we get:

$$\left(p_{b,dyn} - 2\eta_b \frac{\partial w_b}{\partial z} \right)_{ap} = \left(p_{a,dyn} - 2\eta_a \frac{\partial w_a}{\partial z} \right)_{ap} \tag{5.12}$$

where the subscript 'ap' denotes that the expression in the parentheses should be estimated at the apex of the drop surface. Further, in view of eqs (3.5), (3.6), and (5.10), we introduce dimensionless variables in eq (5.12):

$$\eta_b \left(\tilde{p}_b - 2\frac{\partial \tilde{w}_b}{\partial \tilde{z}} \right)_{ap} = \eta_a \left(\tilde{p}_a - 2\frac{\partial \tilde{w}_a}{\partial \tilde{z}} \right)_{ap} \tag{5.13}$$

For the computations, it is convenient to express $\tilde{p}_a$ in the form:

$$\tilde{p}_a(\mathbf{r}) = \tilde{p}_{a,0}(\mathbf{r}) + \left(\tilde{p}_a - 2\frac{\partial \tilde{w}_a}{\partial \tilde{z}} \right)_{ap} \tag{5.14}$$

where the last term in the parentheses is a constant. In fact, Eq. (5.14) represents the definition of $\tilde{p}_{a,0}(\mathbf{r})$. At the apex of the drop surface, Eq. (5.14) gives the boundary condition for $\tilde{p}_{a,0}$:

$$\tilde{p}_{a,0}\Big|_{ap} = 2\frac{\partial \tilde{w}_a}{\partial \tilde{z}}\Bigg|_{ap} \tag{5.15}$$

In view of Eq. (5.9) and (5.14), we obtain:

$$f_a = f_{a,0} + \pi \left(\tilde{p}_a - 2\frac{\partial \tilde{w}_a}{\partial \tilde{z}} \right)_{ap} = f_{a,0} + \frac{\eta_b}{\eta_a} \pi \left(\tilde{p}_b - 2\frac{\partial \tilde{w}_b}{\partial \tilde{z}} \right)_{ap} \tag{5.16}$$

$$\text{where} \quad f_{a,0} = 2\pi \int_0^1 \tilde{p}_{a,0}\, \tilde{r}\, d\tilde{r} \tag{5.17}$$

In Eq. (5.16), at the last step we have used Eq. (5.13). Thus, in view of Eqs. (5.5) and (5.16), we can express the total hydrodynamic force exerted on the drop in the form:

$$F_h = F_a + F_b = f_h \eta_a R_p v_m \tag{5.18}$$

where

$$f_h \equiv f_{a,0}(\alpha) + \frac{\eta_b}{\eta_a} \left[f_b(\alpha) + f_{ab}(\alpha) \right] \tag{5.19}$$

$$f_{ab} = \pi \left(\tilde{p}_b - 2\frac{\partial \tilde{w}_b}{\partial \tilde{z}} \right)_{ap} \tag{5.20}$$

Numerical results and interpolation formulas for are given in section 7 below. Note, that the coefficients $f_{a,0}$, f_b and f_{ab} depend only on the contact angle, α, because of the appropriate scaling procedure given in Section 3. In contrast, the hydrodynamic friction coefficient, f_h, is a

linear function of the ratio between the dynamic viscosities of phases "b" and "a", i.e. of η_b/η_a, see eq. (5.19).

5.2. Introduction of new variables

To avoid numerical problems in calculation of the pressures, p_a and p_b, and the friction coefficients, f_a and f_b, it is convenient to introduce new variables, Ψ_f and Ω_f (f = a, b), as follows:

$$\psi_a \equiv -\tilde{r} + \frac{\tilde{r}^3}{2} + \Psi_a + \tilde{z}\,\Omega_a\,, \quad \omega_a \equiv 4\tilde{r} + 2\frac{\partial \Omega_a}{\partial \tilde{z}} \tag{5.21}$$

$$\psi_b \equiv \Psi_b + \tilde{z}\,\Omega_b\,, \qquad \omega_b \equiv 2\frac{\partial \Omega_b}{\partial \tilde{z}} \tag{5.22}$$

In view of Eq. (4.2), equation (5.21) defines Ψ_a and Ω_a as deviations from the Poiseuille flow in the cylindrical channel of the pore, near its orifice. In addition, in terms of the new variables, equation (3.12) acquires a simpler form:

$$L[\Psi_f] = 0\,, \quad L[\Omega_f] = 0 \qquad (f = a, b) \tag{5.23}$$

in which both equations for Ψ_f and Ω_f are separated one from the others.

Further, substituting ω_a and ω_b from Eqs. (5.21) and (5.22) into Eq. (3.14), and integrating with respect to z, we derive:

$$\tilde{p}_{a,0} = -8\tilde{z} - \frac{2}{\tilde{r}}\frac{\partial}{\partial \tilde{r}}(\tilde{r}\,\Omega_a)\,, \quad \tilde{p}_b = -\frac{2}{\tilde{r}}\frac{\partial}{\partial \tilde{r}}(\tilde{r}\,\Omega_b) \tag{5.24}$$

Eq. (5.24) satisfies the requirements to have Poiseuille flow in the depth of the channel, $\tilde{p}_a = -8\tilde{z}$ for $\tilde{z} \to -\infty$, and the hydrodynamic effects to disappear in the depth of the continuous liquid phase, $\tilde{p}_b = 0$ for $\tilde{z} \to +\infty$. Note that the expression for $\tilde{p}_{a,0}$ in Eq. (5.24) satisfies the boundary condition, Eq. (5.15)

Finally, we substitute Eq. (5.24) into Eqs. (5.9) and (5.17) and obtain compact expressions for the force coefficients:

$$f_{a,0} = -4\pi\,\Omega_a(1,0)\,, \quad f_b = 4\pi\,\Omega_b(1,0) \tag{5.25}$$

Here $\Omega_f(1,0) = \Omega_f(\tilde{r} = 1, \tilde{z} = 0)$ and f = a, b; to derive Eq. (5.25), we have used also the boundary condition $\Omega_b(\infty,0) = 0$. To calculate f_{ab}, we use Eq. (5.20), where

$$\tilde{p}_b\Big|_{ap} = -4\frac{\partial \Omega_b}{\partial \tilde{r}}\bigg|_{ap} \tag{5.26}$$

$$-\left.\frac{\partial \widetilde{w}_{\mathrm{b}}}{\partial \widetilde{z}}\right|_{\mathrm{ap}} = \frac{(1+\cos\alpha)\sin\alpha}{(1-\cos\alpha)\alpha}(\sin\alpha - \alpha\cos\alpha) \tag{5.27}$$

Our next goal is to solve the hydrodynamic problem numerically and, in particular, to compute $\Omega_a(1,0)$ and $\Omega_b(1,0)$.

6. Solution of the problem in curvilinear coordinates

6.1. Coordinate transformations

It is convenient to transform the physical space, occupied by the two liquid phases, including the emulsion drop, into a finite rectangular domain. For this goal, we consider three separate domains (Fig. 2): Domain A represents the interior of the cylindrical capillary. Domain B is the interior of the emulsion drop. Domain C is the outer liquid phase (the disperse medium).

In the domain A, it is convenient to replace the cylindrical coordinates $(\widetilde{r},\widetilde{z})$ by curvilinear coordinates (x_1,x_2), defined as follows:

$$x_1 \equiv \widetilde{r}\,, \quad x_2 \equiv \frac{\widetilde{z}}{1-\widetilde{z}} \tag{6.1}$$

Thus, the domain A, which corresponds to $0 \le \widetilde{r} \le 1$ and $-\infty \le \widetilde{z} \le 0$, is transformed into a finite rectangle, for which $0 \le x_1 \le 1$ and $-1 \le x_2 \le 0$ (Fig. 2). The coordinate surfaces x_1 = const. are vertical cylinders, while the coordinate surfaces x_2 = const. are horizontal planes.

Because the domains B and C are separated by a spherical phase boundary (the drop surface), it is convenient to introduce toroidal coordinates in these two regions:

$$\widetilde{r} \equiv \frac{2x_1}{h}, \quad \widetilde{z} \equiv \frac{1-x_1^2}{h}\sin x_2 \tag{6.2}$$

$$h \equiv 1 + x_1^2 + (1-x_1^2)\cos x_2 \tag{6.3}$$

In this case, the coordinate surfaces x_1 = const. are toroids, while the surfaces x_2 = const. are spheres (Fig. 2). The latter obey the equation:

$$\widetilde{r}^{\,2} + (\widetilde{z} + \cot x_2)^2 = \frac{1}{\sin^2 x_2} \tag{6.4}$$

One could check that (irrespective of the value of x_2) all spheres described by Eq. (6.4) are passing through the circumference $(\widetilde{r}=1, \widetilde{z}=0)$, which is the edge at the orifice of the pore. The drop surface is a sphere, whose dimensionless radius is $\widetilde{R}_{\mathrm{s}} \equiv R_{\mathrm{s}}/R_{\mathrm{p}} = 1/\sin\alpha$ (Fig. 1). Comparing the latter result with the right-hand side of Eq. (6.4), we find that $x_2 = \alpha$ for the

drop surface, which serves as boundary between the domains B and C. In addition, the boundary between the domains A and B corresponds to $x_2 = 0$; see Eqs. (6.1), (6.2) and Fig. 2. Thus, the domain B represents a rectangle, for which $0 \le x_1 \le 1$ and $0 \le x_2 \le \alpha$, whereas for the domain C we have $0 \le x_1 \le 1$ and $\alpha \le x_2 \le \pi$.

The introduced curvilinear coordinates are convenient, because the boundary conditions are imposed on coordinate surfaces. In the next subsections we specify the form of the differential equations and boundary conditions for the domains A, B, and C.

6.2. Domain A

As mentioned above, the domain A is a rectangle for which $0 \le x_1 \le 1$ and $-1 \le x_2 \le 0$ (Fig. 2). Using the curvilinear coordinates defined by Eq. (6.1), we derive:

$$\frac{\partial f}{\partial \tilde{r}} = \frac{\partial f}{\partial x_1}, \quad \frac{\partial f}{\partial \tilde{z}} = (1 + x_2)^2 \frac{\partial f}{\partial x_2} \tag{6.5}$$

In the domain A, we can express the linear differential operator L, defined by Eq. (3.13), as $L = L_1 + L_2$, where

$$L_1[f] = \frac{\partial^2 f}{\partial x_1^2} + \frac{1}{x_1}\frac{\partial f}{\partial x_1} - \frac{f}{x_1^2} \tag{6.6}$$

$$L_2[f] = (1 + x_2)^4 \frac{\partial^2 f}{\partial x_2^2} + 2(1 + x_2)^3 \frac{\partial f}{\partial x_2} \tag{6.7}$$

Note that the expression for L in the domains B and C is different; see Eqs. (6.14) and (6.15). The unknown functions, Ψ_a and Ω_a, satisfy Eqs. (5.23). Our next task is to obtain the respective boundary conditions at the borders of the domain A.

At the axis of symmetry, $\tilde{r} = 0$, which corresponds to $x_1 = 0$, with the help of Eqs. (4.1) and (5.21), we obtain:

$$\Psi_a = \Omega_a = 0 \quad \text{at} \quad x_1 = 0 \ \text{and} \ -1 \le x_2 \le 0 \tag{6.8}$$

In the depth of the capillary channel, far from its orifice, $\tilde{z} \to -\infty$, $x_2 = -1$, from Eqs. (4.2) and (5.21) we derive:

$$\Psi_a = \Omega_a = 0 \quad \text{at} \quad 0 \le x_1 \le 1 \ \text{and} \ x_2 = -1 \tag{6.9}$$

At the solid wall of the cylindrical channel $(\tilde{r} = 1)$, corresponding to $x_1 = 1$, with the help of Eqs. (4.3), (5.21), (6.1), and (6.5) we obtain:

$$\Psi_a + \frac{x_2}{1 + x_2}\Omega_a = 0, \quad \frac{\partial \Psi_a}{\partial x_1} + \frac{x_2}{1 + x_2}\frac{\partial \Omega_a}{\partial x_1} = 0 \tag{6.10}$$

at $x_1 = 1$ and $-1 < x_2 \le 0$. Finally, the boundary condition at the border between domains A and B (Fig. 2) is derived in the next subsection.

6.3. Domain B

The domain B, representing the interior of the forming drop at the opening of the channel, corresponds to $0 \le x_1 \le 1$ and $0 \le x_2 \le \alpha$ (see Fig. 2). From the definition of the toroidal coordinates, Eq. (6.2), it follows that

$$\frac{\partial \tilde{r}}{\partial x_1} = \frac{2}{h^2}[(1-x_1^2)+(1+x_1^2)\cos x_2], \quad \frac{\partial \tilde{z}}{\partial x_2} = \frac{1-x_1^2}{2}\frac{\partial \tilde{r}}{\partial x_1} \tag{6.11}$$

$$\frac{\partial \tilde{r}}{\partial x_2} = \frac{2}{h^2}x_1(1-x_1^2)\sin x_2, \quad \frac{\partial \tilde{z}}{\partial x_1} = -\frac{2}{1-x_1^2}\frac{\partial \tilde{r}}{\partial x_2} \tag{6.12}$$

The respective metric coefficients (Lamé parameters) are:

$$h_1 = \frac{2}{h}, \quad h_2 = \frac{1-x_1^2}{h} \tag{6.13}$$

With the help of Eqs. (3.13), (6.2) and (6.11)-(6.13), one can express the differential operator $L = L_1 + L_2$ in terms of the toroidal coordinates (x_1,x_2):

$$L_1[f] = \frac{h^2}{4}\frac{\partial^2 f}{\partial x_1^2} + (\frac{h^2}{4x_1} - \frac{x_1 h}{1-x_1^2})\frac{\partial f}{\partial x_1} - \frac{h^2}{4x_1^2} f \tag{6.14}$$

$$L_2[f] = \frac{h^2}{(1-x_1^2)^2}\frac{\partial^2 f}{\partial x_2^2} + \frac{h\sin x_2}{1-x_1^2}\frac{\partial f}{\partial x_2} \tag{6.15}$$

Two other useful relationships connect the derivatives in terms of the cylindrical and toroidal coordinates:

$$\frac{\partial f}{\partial \tilde{r}} = \frac{1}{2}[(1-x_1^2)+(1+x_1^2)\cos x_2]\frac{\partial f}{\partial x_1} + \frac{2x_1 \sin x_2}{1-x_1^2}\frac{\partial f}{\partial x_2} \tag{6.16}$$

$$\frac{\partial f}{\partial \tilde{z}} = -x_1 \sin x_2 \frac{\partial f}{\partial x_1} + (1+\frac{1+x_1^2}{1-x_1^2}\cos x_2)\frac{\partial f}{\partial x_2} \tag{6.17}$$

Our next step is to derive the boundary conditions at the borders of the domain B.

At the axis of symmetry, $\tilde{r} = 0$, which corresponds to $x_1 = 0$ (see Fig. 2), in view of Eqs. (4.1) and (5.21) we obtain:

$$\Psi_a = \Omega_a = 0 \quad \text{at } x_1 = 0 \text{ and } 0 \le x_2 \le \alpha \tag{6.18}$$

Furthermore, at the edge of the pore, $\tilde{r} = 1$, $\tilde{z} = 0$ ($x_1 = 1$, $0 \le x_2 \le \alpha$, see Fig. 2), that is at the three-phase contact line, from Eqs. (4.3) and (5.21) one deduces (see Appendix B):

$$\Psi_a = 0, \quad \frac{\partial \Psi_a}{\partial x_1} - \Omega_a \sin x_2 = 0 \quad \text{at } x_1 = 1 \text{ and } 0 \le x_2 \le \alpha \tag{6.19}$$

The boundary between the domains A and B at $x_2 = 0$ is formal: there is no physical boundary there. For this reason, the functions Ψ_a, Ω_a, and their directional (normal) derivatives must be discontinuous at this boundary:

$$\Psi_a\big|_{x_2=0-0} = \Psi_a\big|_{x_2=0+0}, \quad \left.\frac{\partial \Psi_a}{\partial x_2}\right|_{x_2=0-0} = \frac{2}{1-x_1^2}\left.\frac{\partial \Psi_a}{\partial x_2}\right|_{x_2=0+0} \tag{6.20}$$

$$\Omega_a\big|_{x_2=0-0} = \Omega_a\big|_{x_2=0+0}, \quad \left.\frac{\partial \Omega_a}{\partial x_2}\right|_{x_2=0-0} = \frac{2}{1-x_1^2}\left.\frac{\partial \Omega_a}{\partial x_2}\right|_{x_2=0+0} \tag{6.21}$$

for every $0 \le x_1 \le 1$, see Eqs. (6.5) and (6.17).

Next, let us consider the boundary conditions at the drop surface (the oil-water interface), where $x_2 = \alpha$. Using definition (5.21), after some mathematical transformations, one can express boundary conditions (4.5)–(4.7) in the following form (Appendix B):

$$\Psi_a + \tilde{z}\,\Omega_a = [1-(1-x_1^2)\cos\alpha]\frac{\tilde{r}}{2} - \frac{\tilde{r}^3}{2} \tag{6.22}$$

$$\frac{h}{1-x_1^2}\frac{\partial \Psi_a}{\partial x_2} + \sin\alpha \frac{\partial \Omega_a}{\partial x_2} + [(1-x_1^2)+(1+x_1^2)\cos\alpha]\frac{\Omega_a}{h} = \sin\alpha \frac{1+\cos\alpha}{1-\cos\alpha}s +$$

$$+[(1-x_1^2)\cos\alpha + \frac{1-5\cos\alpha}{1-\cos\alpha}]\frac{\sin\alpha}{2}\tilde{r} - \frac{3\sin\alpha}{2}\tilde{r}^3 \tag{6.23}$$

where $x_2 = \alpha$, $0 \le x_1 \le 1$, and $\tilde{r}$ and $\tilde{z}$ are defined by Eq. (6.2).

6.3. Domain C

In this domain, the unknown hydrodynamic functions are Ψ_b and Ω_b. For domains B and C we have the same curvilinear coordinates, Eq. (6.2), and consequently, Ψ_b and Ω_b must satisfy Eqs. (5.23), where the differential operator $L = L_1 + L_2$ is defined by Eqs. (6.14) and (6.15). At the axis of symmetry, $\tilde{r} = 0$, which corresponds to $x_1 = 0$ (see Fig. 2), in analogy with Eq. (6.8) we obtain:

$$\Psi_b = \Omega_b = 0 \quad \text{at } x_1 = 0 \text{ and } \alpha \le x_2 \le \pi \tag{6.24}$$

Furthermore, at the edge of the pore, $\tilde{r} = 1$, $\tilde{z} = 0$ ($x_1 = 1$, $\alpha \le x_2 \le \pi$, see Fig. 2), that is at the three-phase contact line, from Eqs. (4.4) and (5.22) in toroidal coordinates (6.2) one deduces (Appendix B):

$$\Psi_b = -\frac{1}{2}, \quad \frac{\partial \Psi_b}{\partial x_1} - \Omega_b \sin x_2 = \frac{1}{2}\cos x_2 \qquad \text{at } x_1 = 1 \text{ and } \alpha \le x_2 \le \pi \tag{6.25}$$

At the outer membrane wall, where $\tilde{z} = 0$ and $x_2 = \pi$ (Fig. 2), we derive the following boundary condition with the help of Eqs. (4.4), (5.22), (6.2), (6.3) and (6.17):

$$\Psi_b = -\frac{x_1}{2}, \quad \frac{2x_1^2}{1-x_1^2}\frac{\partial \Psi_b}{\partial x_2} - \Omega_b = 0 \qquad \text{at } 0 \le x_1 \le 1 \text{ and } x_2 = \pi \tag{6.26}$$

To derive the boundary condition at the surface of the drop ($x_2 = \alpha$), we transform Eqs. (4.5) and (4.6) with the help of definitions (5.22) in terms of the new functions Ψ_b and Ω_b (Appendix B):

$$\Psi_b + \tilde{z}\,\Omega_b = -[1 + (1-x_1^2)\cos\alpha]\frac{\tilde{r}}{2} \tag{6.27}$$

$$\frac{h}{1-x_1^2}\frac{\partial \Psi_b}{\partial x_2} + \sin\alpha \frac{\partial \Omega_b}{\partial x_2} + [(1-x_1^2) + (1+x_1^2)\cos\alpha]\frac{\Omega_b}{h} = \frac{1+\cos\alpha}{1-\cos\alpha} s \sin\alpha +$$

$$+ [(1-x_1^2)\cos\alpha - \frac{1+3\cos\alpha}{1-\cos\alpha}]\frac{\sin\alpha}{2}\tilde{r} \tag{6.28}$$

where $x_2 = \alpha$, $0 \le x_1 \le 1$, and $\tilde{r}$ and $\tilde{z}$ are defined by Eq. (6.2).

7. Numerical results and discussion

We solved the problem numerically. The three integration domains, A, B, and C, were transformed into rectangles with the help of appropriate curvilinear coordinates, (x_1,x_2), as explained in section 6 (Fig. 2). The boundary conditions at the borders of each rectangle, and the expressions for the differential operator, L, are also given in section 6. As a result, we obtained numerical data for the functions $\Psi_f(x_1,x_2)$ and $\Omega_f(x_1,x_2)$, f = a,b. We recall, that the subscript 'a' denotes the inner (disperse) phase, while the subscript 'b' denotes the outer (continuous) phase. Next, from Eqs. (5.10) and (5.11) we determined the stream and vorticity functions $\psi_f(x_1,x_2)$ and $\omega_f(x_1,x_2)$, f = a,b. Finally, from Eq. (3.10) we calculated the radial and vertical components of the velocity field, $\tilde{u}_f(x_1, x_2)$ and $\tilde{w}_f(x_1, x_2)$, f = a,b. In addition, from Eq. (5.25)–(5.27) we determined the coefficients, $f_{a,0}$, f_b, and f_{ab}, which characterize the hydrodynamic force, F_h, that is acting on the emulsion drop; see also Eq. (5.18).

It is worthwhile noting that the obtained numerical data for the dimensionless characteristics of the system (Figs. 3–6) have universal character: They depend only on the angle α (Fig. 1), determining the drop size relative to the pore size, but they are independent of the pore radius, R_p; of the mean velocity of the fluid in the channel, v_m, and of the viscosities of the two fluid phases, η_a and η_b.

As an illustration, in Figs. 3–7 we show the calculated stream function, ψ, dimensionless radial velocity component, v_r, and dimensionless vertical velocity component, v_z, for angles $\alpha = 30°$, 60°, 90°, 120°, and 150°. The boundary between the domains A and B is always at $x_2 = 0$. In Figs. 3–7, the used scale of the colors is the same, which allow one to compare the magnitudes of the respective quantities for the various values of α.

The curvilinear coordinates, (x_1,x_2), are convenient for the numerical calculations, but they are not convenient for data presentation, because they distort the shape of the emulsion drop. For this reason, in Fig. 8 we have recalculated the velocity profile by using polar coordinates with coordinate origin at the center of the sphere, representing the drop surface. For convenience, the velocity field, **v**, is plotted in Cartesian coordinates, where, as usual, the z-axis coincides with the axis of symmetry of the system. Figure 8a corresponds to $R_s/R_p = 1/\sin\alpha = 1.1$ ($\alpha \approx 115°$), while Fig. 8b corresponds to $R_s/R_p = 1.3$ ($\alpha \approx 130°$). The general pattern of the velocity field in Fig. 8 does not show the existence of vorticity structures inside the drop. The flow is predominantly directed out of the pore, along the z-axis, with a superimposed additional radial flow, engendered by the radial expansion of the drop surface. We recall that the used boundary conditions at the drop surface, Eqs. (2.9) and (2.10), physically correspond to an oil-water interface that expands isotropically as an elastic membrane. Such a kinematic regime is expected when adsorbed surfactant is present at the interface: the surfactant gives rise to a considerable surface dilatational (Gibbs) elasticity.

Figures 9a and 9b show the calculated hydrodynamic-force coefficients, $f_{a,0}$, f_b and f_{ab} as universal functions of the angle α. Physically, $f_{a,0}$ and f_{ab} characterizes the "pushing" force that originates from the inner fluid, which is ejected from the orifice of the pore. The most interesting results are that the dependence $f_{a,0}(\alpha)$ exhibits a maximum. In other words, the emulsion drop, which is forming at the opening of the pore, experiences a strong pushing force from the side of the inner fluid, which eventually could lead to detachment of the drop from the membrane surface. On the other hand, the hydrodynamic force coefficient f_b is negative, and characterizes the drag force that originates from the outer fluid and impedes the growth of the drop, see Eq. 5.18.

Appendix A. Calculation of boundary conditions (4.5) and (4.6)

From equations (2.14) and (3.10) the normal component of the velocity at the drop surface is presented as:

$$\mathbf{n}\cdot\widetilde{\mathbf{v}}_{\mathrm{f}} = \sin\theta\frac{\partial\psi_{\mathrm{f}}}{\partial\widetilde{z}} - \cos\theta\frac{\partial\psi_{\mathrm{f}}}{\partial\widetilde{r}} - \frac{\cos\theta}{\widetilde{r}}\psi_{\mathrm{f}} \tag{A.1}$$

where f = a, b. Equation (A.1) is simplified using the spherical coordinate system connected to the drop center, O_{s}, with dimensionless coordinates $(\widetilde{r}_{\mathrm{sph}},\theta)$:

$$\widetilde{r} = \widetilde{r}_{\mathrm{sph}}\sin\theta, \quad \widetilde{z} = \widetilde{z}_{\mathrm{d}} + \widetilde{r}_{\mathrm{sph}}\cos\theta \tag{A.2}$$

In the spherical coordinates (A.2) equation (A.1) is transformed to:

$$\mathbf{n}\cdot\widetilde{\mathbf{v}}_{\mathrm{f}} = -\frac{1}{\widetilde{r}_{\mathrm{sph}}\sin\theta}\frac{\partial}{\partial\theta}(\psi_{\mathrm{f}}\sin\theta) \tag{A.3}$$

From Eq. (3.5) the dimensionless spherical coordinate at the drop surface is equal to $\widetilde{r}_{\mathrm{sph}} = 1/\sin\alpha$. Using the expression for the normal velocity component at the drop surface, Eq. (2.12), equation (A.3) reduces to the following relationship:

$$\frac{\partial}{\partial\theta}(\psi_{\mathrm{f}}\sin\theta) = -\frac{1+\cos\alpha}{1-\cos\alpha}(\cos\theta-\cos\alpha)\frac{\sin\theta}{\sin\alpha} \tag{A.4}$$

The differential equation (A.4) is integrated with respect to the polar angle from 0 to θ and the result reads

$$\psi_{\mathrm{f}}\sin\theta = \frac{1}{\sin\alpha}\frac{1+\cos\alpha}{1-\cos\alpha}\left[\frac{\cos^2\theta-1}{2} - \cos\alpha(\cos\theta-1)\right] \tag{A.5}$$

Simple mathematical calculations reduce equation (A.5) to its equivalent form:

$$\psi_{\mathrm{f}} = -\frac{1}{2}\frac{1+\cos\alpha}{1-\cos\alpha}\frac{\sin\theta}{\sin\alpha}\left(1-\frac{2\cos\alpha}{1+\cos\theta}\right) \tag{A.6}$$

It is important to note that the stream function (A.6) is continuous at the contact line, i.e. the value of ψ_{f} is equal to –1/2 at $\theta = \alpha$, see also Eqs. (4.3) and (4.4).

From equations (2.14) and (3.10) the tangential component of the velocity at the drop surface is calculated:

$$\mathbf{t}\cdot\widetilde{\mathbf{v}}_{\mathrm{f}} = \cos\theta\frac{\partial\psi_{\mathrm{f}}}{\partial\widetilde{z}} + \sin\theta\frac{\partial\psi_{\mathrm{f}}}{\partial\widetilde{r}} + \frac{\sin\theta}{\widetilde{r}}\psi_{\mathrm{f}} \tag{A.7}$$

where f = a, b. Expression (A.7) is reduced at the drop surface to [see Eq. (A.2)]:

$$\mathbf{t}\cdot\widetilde{\mathbf{v}}_{\mathrm{f}} = \sin\theta\frac{\partial\psi_{\mathrm{f}}}{\partial\widetilde{r}} + \cos\theta\frac{\partial\psi_{\mathrm{f}}}{\partial\widetilde{z}} + \psi_{\mathrm{f}}\sin\alpha \tag{A.8}$$

The sum of partial derivatives in Eq. (A.8) is equal to the directional (normal) derivative of the stream function at the drop surface.

Appendix B. Calculation of boundary conditions (6.19), (6.22), (6.23), (6.25), (6.27) and (6.28)

Boundary condition (6.19). If definitions (5.21) are substituted into Eq. (3.10) the following expressions for the velocity components are derived:

$$\widetilde{u}_{\mathrm{a}} = \frac{\partial \Psi_{\mathrm{a}}}{\partial \widetilde{z}} + \widetilde{z}\frac{\partial \Omega_{\mathrm{a}}}{\partial \widetilde{z}} + \Omega_{\mathrm{a}} \tag{B.1}$$

$$\widetilde{w}_{\mathrm{a}} = -(\frac{\partial \Psi_{\mathrm{a}}}{\partial \widetilde{r}} + \widetilde{z}\frac{\partial \Omega_{\mathrm{a}}}{\partial \widetilde{r}}) - \frac{1}{\widetilde{r}}(\Psi_{\mathrm{a}} + \widetilde{z}\Omega_{\mathrm{a}}) + 2(1-\widetilde{r}^{\,2}) \tag{B.2}$$

The velocity component in direction x_2 is calculated using the metric coefficients (6.13) to be:

$$\widetilde{\mathbf{v}}_{\mathrm{f}} \cdot \mathbf{e}_2 = \frac{h}{1-x_1^2}\frac{\partial \widetilde{r}}{\partial x_2}\widetilde{u}_{\mathrm{f}} + \frac{h}{1-x_1^2}\frac{\partial \widetilde{z}}{\partial x_2}\widetilde{w}_{\mathrm{f}} \qquad (\mathrm{f} = \mathrm{a}, \mathrm{b}) \tag{B.3}$$

Expressions (B.1) and (B.2) are substituted into Eq. (B.3) and formulas (6.11) and (6.12) are used in order to obtain the relationship for the velocity component in terms of unknown functions Ψ_{a} and Ω_{a}:

$$\widetilde{\mathbf{v}}_{\mathrm{a}} \cdot \mathbf{e}_2 = -\frac{h}{2}(\frac{\partial \Psi_{\mathrm{a}}}{\partial x_1} + \widetilde{z}\frac{\partial \Omega_{\mathrm{a}}}{\partial x_1}) + \frac{h}{2}\frac{\partial \widetilde{r}}{\partial x_1}[2(1-\widetilde{r}^{\,2}) - \frac{1}{\widetilde{r}}(\Psi_{\mathrm{a}} + \widetilde{z}\Omega_{\mathrm{a}})] - \frac{h}{2}\frac{\partial \widetilde{z}}{\partial x_1}\Omega_{\mathrm{a}} \tag{B.4}$$

To derive boundary condition (6.19) we apply Eq. (B.4) at the contact line, where $\widetilde{r} = 1$, $\widetilde{z} = 0$ and x_1 =1. From Eq. (6.12) it follows that at the contact line:

$$\frac{\partial \widetilde{z}}{\partial x_1} = -\frac{4x_1}{h^2}\sin x_2 \to -\sin x_2 \qquad \text{at } x_1 \to 1 \tag{B.5}$$

and the velocity component becomes:

$$\widetilde{\mathbf{v}}_{\mathrm{a}} \cdot \mathbf{e}_2 = -\frac{\partial \Psi_{\mathrm{a}}}{\partial x_1} + \Omega_{\mathrm{a}}\sin x_2 \qquad \text{at } x_1 = 1 \tag{B.6}$$

The velocity of the liquid at the contact line is zero and Eq. (B.6) gives boundary condition (6.19).

Boundary condition (6.22). The substitution of Eq. (5.21) into boundary condition (4.5) leads to the following relationship:

$$\Psi_{\mathrm{a}} + \widetilde{z}\Omega_{\mathrm{a}} = \widetilde{r} - \frac{\widetilde{r}^{\,3}}{2} - \frac{1}{2}(1 - \frac{2\cos\alpha}{1+\cos\theta})\frac{1+\cos\alpha}{1-\cos\alpha}\frac{\sin\theta}{\sin\alpha} \tag{B.7}$$

written at $x_2 = \alpha$. Using Eq. (A.2) the radial and vertical coordinates at the drop surface are simply related to the polar angle:

$$\widetilde{r} = \frac{\sin\theta}{\sin\alpha}, \quad \widetilde{z} = \frac{\cos\theta - \cos\alpha}{\sin\alpha} \tag{B.8}$$

From Eqs. (6.2) and (6.3) we can find $\widetilde{z}$ and replace it into Eq. (B.8) to obtain the cosine of the polar angle:

$$\cos\theta = \frac{1 - x_1^2}{1 + x_1^2 + (1 - x_1^2)\cos\alpha}\sin^2\alpha + \cos\alpha = \frac{1 - x_1^2 + (1 + x_1^2)\cos\alpha}{1 + x_1^2 + (1 - x_1^2)\cos\alpha} \tag{B.9}$$

After equivalent mathematical transformation it can be calculated from Eq. (B.9) that:

$$\frac{1 + \cos\alpha}{1 + \cos\theta} = \frac{1}{2}[1 + x_1^2 + (1 - x_1^2)\cos\alpha] \tag{B.10}$$

The direct substitution of Eq. (B.10) and (B.8) into boundary condition (B.7) reduces it to Eq. (6.22).

Boundary condition (6.23). The directional (normal) derivative of the stream function, appearing in boundary condition (4.6)-(4.7) is presented for new functions (5.21) in the following form:

$$\frac{\partial\psi_a}{\partial n} = (\frac{3\widetilde{r}^2}{2} - 1)\sin\theta + \Omega_a\cos\theta + \sin\theta\frac{\partial\Psi_a}{\partial\widetilde{r}} + \cos\theta\frac{\partial\Psi_a}{\partial\widetilde{z}} +$$

$$+ \widetilde{z}(\sin\theta\frac{\partial\Omega_a}{\partial\widetilde{r}} + \cos\theta\frac{\partial\Omega_a}{\partial\widetilde{z}}) \tag{B.11}$$

From Eqs. (B.8) and (B.9) using the expressions for the derivatives $\partial\widetilde{r}/\partial x_2$ and $\partial\widetilde{z}/\partial x_2$, i.e. Eqs. (6.11) and (6.12), the following representations of the trigonometric functions of the polar angle are derived:

$$\sin\theta = \frac{h}{1 - x_1^2}\frac{\partial\widetilde{r}}{\partial x_2} \quad \text{and} \quad \cos\theta = \frac{h}{1 - x_1^2}\frac{\partial\widetilde{z}}{\partial x_2} \tag{B.12}$$

Finally, from Eqs. (B.8), (B.9) and (B.12) the normal derivative of the stream function (B.11) is simplified to:

$$\frac{\partial\psi_a}{\partial n} = \sin\alpha(\frac{3\widetilde{r}^3}{2} - \widetilde{r}) + \frac{1 - x_1^2 + (1 + x_1^2)\cos\alpha}{1 + x_1^2 + (1 - x_1^2)\cos\alpha}\Omega_a + \frac{h}{1 - x_1^2}\frac{\partial\Psi_a}{\partial x_2} + \sin\alpha\frac{\partial\Omega_a}{\partial x_2} \tag{B.13}$$

The following step in calculations is to substitute the values of the stream function from boundary condition (4.5) into boundary condition (4.6) in order to obtain:

$$\frac{\partial\psi_f}{\partial n} = \frac{1 + \cos\alpha}{1 - \cos\alpha}s\sin\alpha - (\frac{1}{2} + \frac{\cos\alpha}{1 + \cos\theta})\frac{1 + \cos\alpha}{1 - \cos\alpha}\sin\theta \qquad (f = a, b) \tag{B.14}$$

Substituting expression (B.13) into Eq. (B.14) written for the phase “a” it is derived that:

$$\frac{h}{1-x_1^2}\frac{\partial \Psi_a}{\partial x_2}+\sin\alpha\frac{\partial \Omega_a}{\partial x_2}+[1-x_1^2+(1+x_1^2)\cos\alpha]\frac{\Omega_a}{h}=-\frac{3\sin\alpha}{2}\tilde{r}^3+$$

$$+\frac{1+\cos\alpha}{1-\cos\alpha}s\sin\alpha-\sin\alpha[(\frac{1}{2}+\frac{\cos\alpha}{1+\cos\theta})\frac{1+\cos\alpha}{1-\cos\alpha}-1]\tilde{r} \qquad \text{(B.15)}$$

Using relationship (B.10) boundary condition (B.15) is transformed to the final form of the boundary condition, i.e. Eq. (6.23).

Boundary condition (6.25). If definitions (5.22) are substituted into Eq. (3.10) the following expressions for the velocity components are derived:

$$\tilde{u}_b=\frac{\partial \Psi_b}{\partial \tilde{z}}+\tilde{z}\frac{\partial \Omega_b}{\partial \tilde{z}}+\Omega_b \qquad \text{(B.16)}$$

$$\tilde{w}_b=-(\frac{\partial \Psi_b}{\partial \tilde{r}}+\tilde{z}\frac{\partial \Omega_b}{\partial \tilde{r}})-\frac{1}{\tilde{r}}(\Psi_b+\tilde{z}\Omega_b) \qquad \text{(B.17)}$$

Expressions (B.16) and (B.17) are substituted into Eq. (B.3) and formulas (6.11) and (6.12) are used in order to obtain the relationship for the velocity component in terms of unknown functions Ψ_b and Ω_b:

$$\tilde{\mathbf{v}}_b\cdot\mathbf{e}_2=-\frac{h}{2}(\frac{\partial \Psi_b}{\partial x_1}+\tilde{z}\frac{\partial \Omega_b}{\partial x_1})-\frac{h}{2\tilde{r}}\frac{\partial \tilde{r}}{\partial x_1}(\Psi_b+\tilde{z}\Omega_b)-\frac{h}{2}\frac{\partial \tilde{z}}{\partial x_1}\Omega_b \qquad \text{(B.18)}$$

To derive boundary condition (6.25) we apply Eq. (B.18) at the contact line, where $\tilde{r}=1$, $\tilde{z}=0$ and x_1 =1. From Eq. (6.11) it follows that at the contact line:

$$\frac{\partial \tilde{r}}{\partial x_1}\to\cos x_2 \qquad \text{at } x_1\to 1 \qquad \text{(B.19)}$$

Using Eqs. (B.5) and (B.19) the velocity component, Eq. (B.18), becomes:

$$\tilde{\mathbf{v}}_b\cdot\mathbf{e}_2=-\frac{\partial \Psi_b}{\partial x_1}-\Psi_b\cos x_2+\Omega_b\sin x_2 \qquad \text{at } x_1\to 1 \qquad \text{(B.20)}$$

Taken into account that the velocity must be zero at the contact line equation (B.20) gives the following boundary condition:

$$\frac{\partial \Psi_b}{\partial x_1}-\Omega_b\sin x_2=-\Psi_b\cos x_2 \qquad \text{at } x_1=1 \qquad \text{(B.21)}$$

Boundary condition (6.27). From Eq. (B.8) the right hand side of Eq. (4.5) is transformed to:

$$\psi_b=-\frac{\tilde{r}}{2}(\frac{1+\cos\alpha}{1-\cos\alpha}-\frac{2\cos\alpha}{1-\cos\alpha}\frac{1+\cos\alpha}{1+\cos\theta}) \qquad \text{(B.22)}$$

Using relationship (B.10) equation (B.22) is simplified:

$$\psi_{\mathrm{b}} = -\frac{\tilde{r}}{2}\left[\frac{1+\cos\alpha}{1-\cos\alpha} - \frac{\cos\alpha}{1-\cos\alpha}(1+\cos\alpha) - x_1^2\cos\alpha\right] \tag{B.23}$$

After simple mathematical transformation of Eq. (B.23) boundary condition (6.27) is calculated.

Boundary condition (6.28). The directional (normal) derivative of the stream function, appearing in boundary condition (4.6)-(4.7) is presented for new functions (5.22) in the following form:

$$\frac{\partial\psi_{\mathrm{b}}}{\partial n} = \frac{h}{1-x_1^2}\frac{\partial\Psi_{\mathrm{b}}}{\partial x_2} + \sin\alpha\frac{\partial\Omega_{\mathrm{b}}}{\partial x_2} + [1-x_1^2+(1+x_1^2)\cos\alpha]\frac{\Omega_{\mathrm{b}}}{h} \tag{B.24}$$

Equation (B.24) follows directly from Eq. (B.13), in which the non-homogeneous term is omitted because of definition (5.22) and the phase "a" is replaced by the phase "b". Applying expressions (B.8) and (B.9) to relationship (B.14) written for the phase "b" it is derived that:

$$\frac{\partial\psi_{\mathrm{b}}}{\partial n} = \frac{1+\cos\alpha}{1-\cos\alpha}s\sin\alpha - \{\frac{1+\cos\alpha}{1-\cos\alpha} + \frac{\cos\alpha}{1-\cos\alpha}[(1+\cos\alpha)+(1-\cos\alpha)x_1^2]\}\frac{\sin\alpha}{2}\tilde{r} \tag{B.25}$$

After equivalent mathematical transformations the right hand side of Eq. (B.25) is simplified to obtain:

$$\frac{\partial\psi_{\mathrm{b}}}{\partial n} = \frac{1+\cos\alpha}{1-\cos\alpha}s\sin\alpha + [(1-x_1^2)\cos\alpha - \frac{1+3\cos\alpha}{1-\cos\alpha}]\frac{\sin\alpha}{2}\tilde{r} \tag{B.26}$$

Equations (B.24) and (B.26) are reduced to boundary condition (6.28).

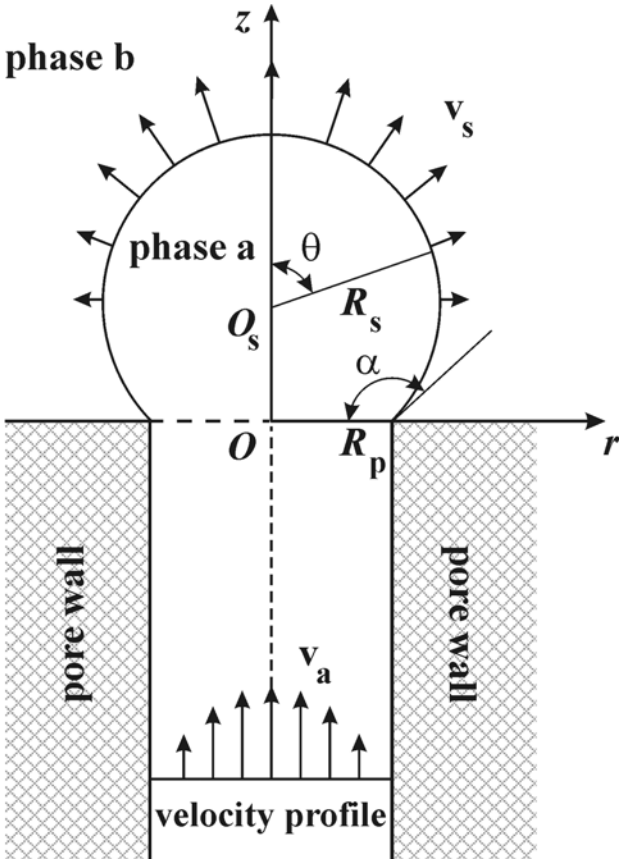

Fig. 1. Drop from the liquid phase 'a' growing at the orifice of a membrane pore. Phase 'b' is the outer liquid medium. R_p and R_s are the radii of the cylindrical pore and spherical drop surface. Angle α characterizes the size of the drop, while angle θ characterizes the position of the material points at the drop surface; $\mathbf{v}_s$ is the surface velocity.

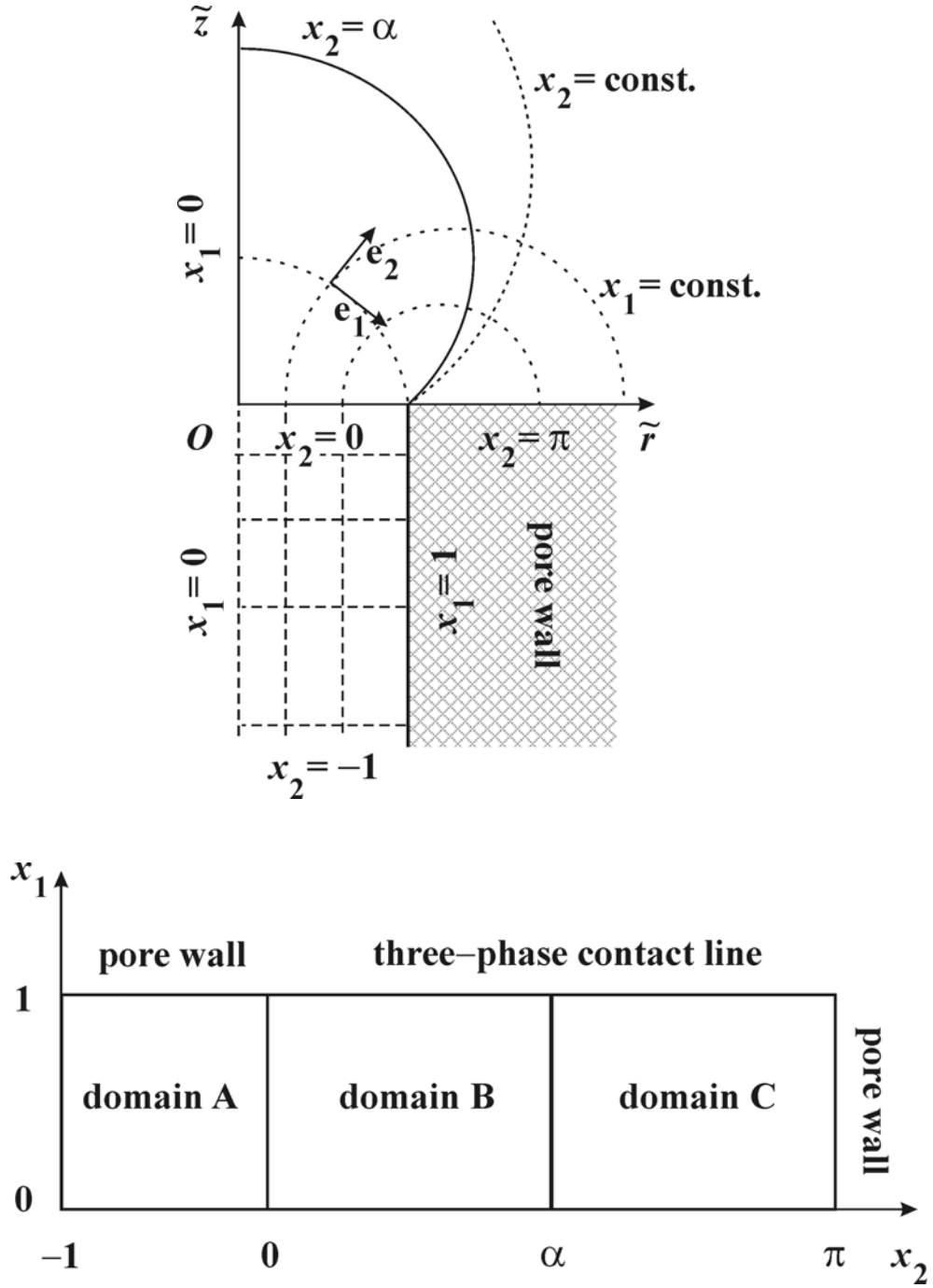

Fig. 2. (a) Curvilinear coordinates (x_1,x_2) introduced in Section 6. (b) The pore interior, drop interior and the outer phase are transformed, respectively, into rectangular domains, A, B, and C.

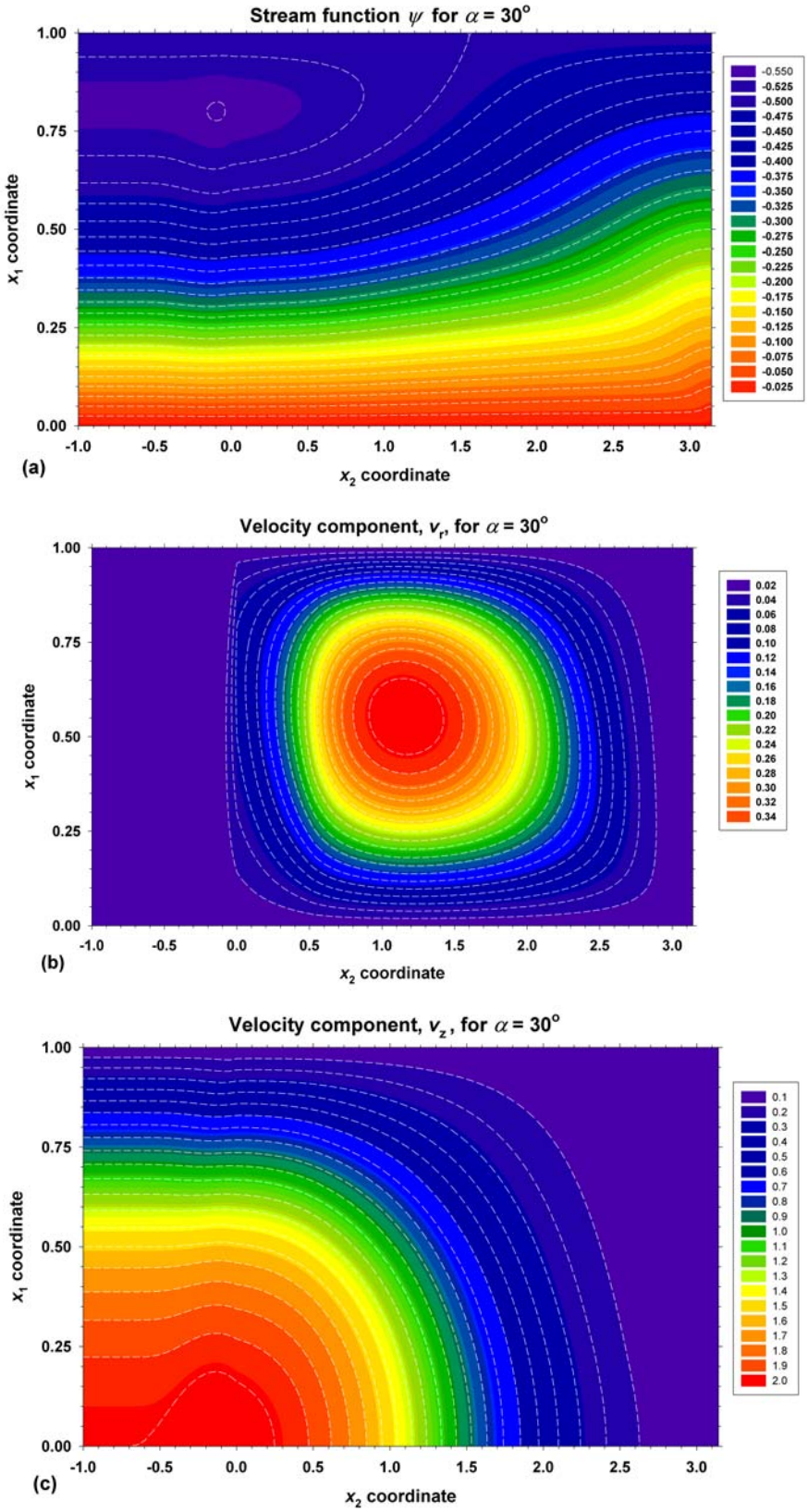

Fig. 3. Calculated (a) stream function, ψ, (b) radial velocity component, v_r, and vertical velocity component, v_z, for angle $\alpha = 30°$.

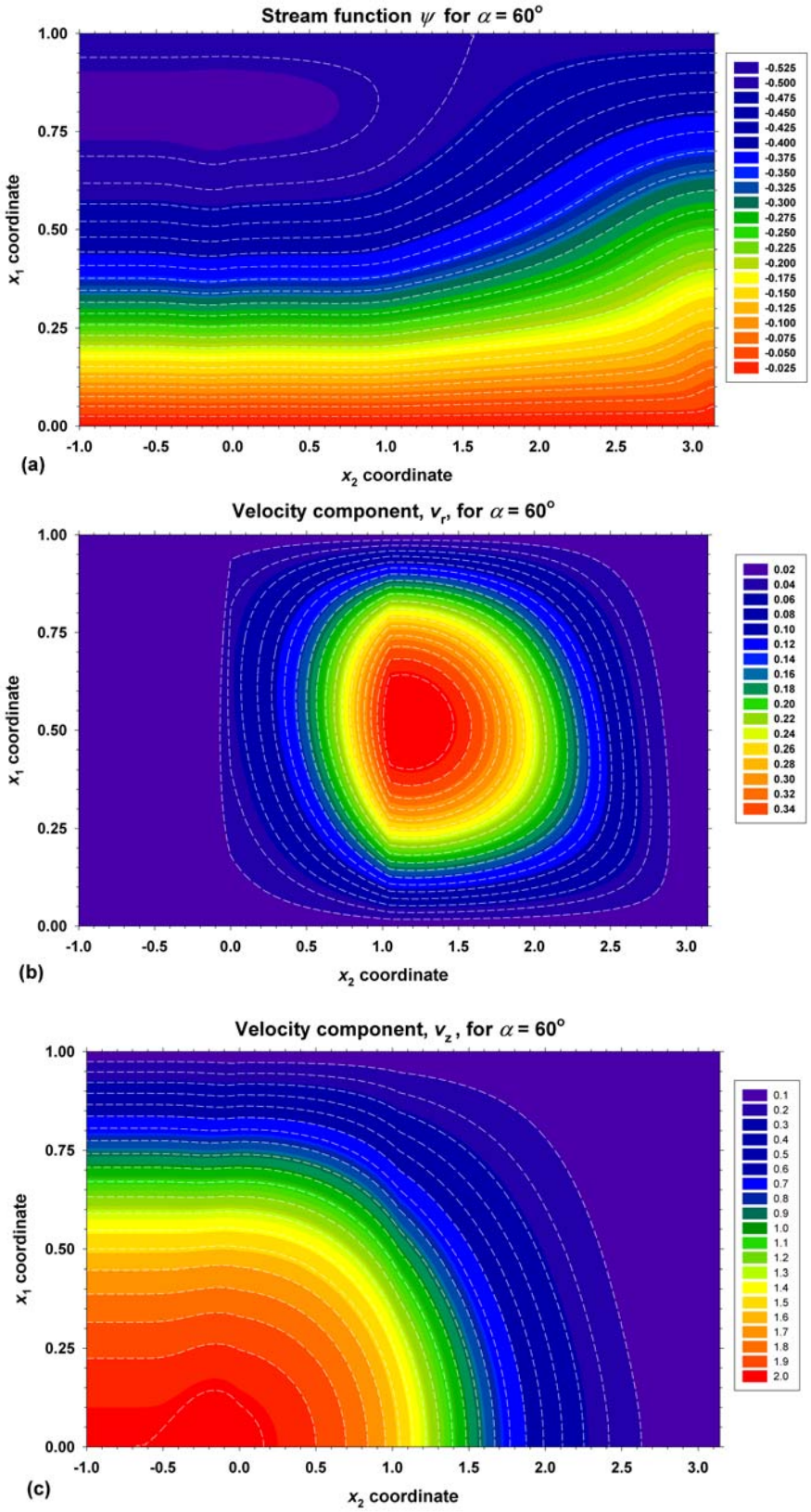

Fig. 4. Calculated (a) stream function, ψ, (b) radial velocity component, v_r, and vertical velocity component, v_z, for angle $\alpha = 60°$.

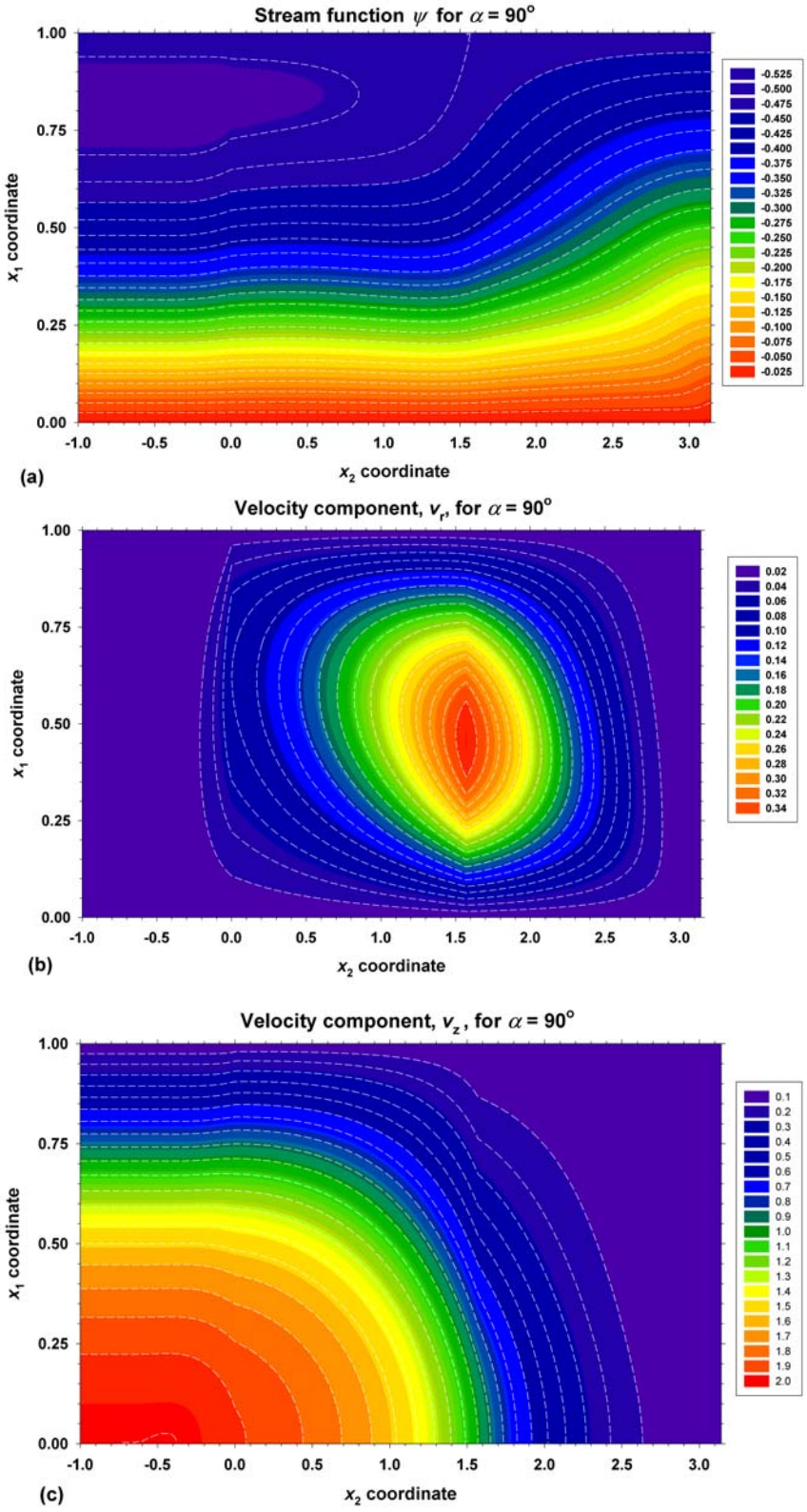

Fig. 5. Calculated (a) stream function, ψ; (b) radial velocity component, v_r, and vertical velocity component, v_z, for angle $\alpha = 90°$.

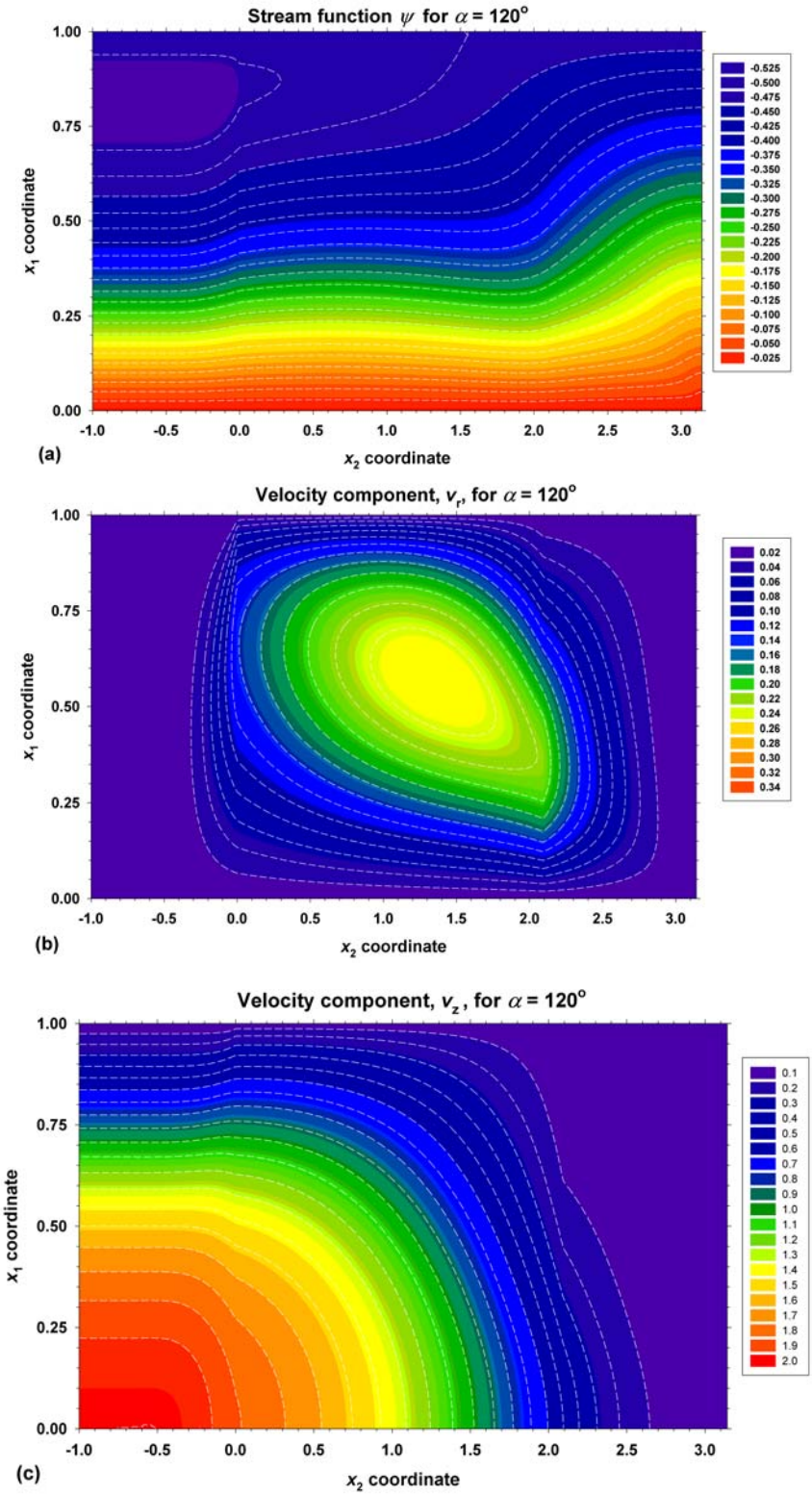

Fig. 6. Calculated (a) stream function, ψ; (b) radial velocity component, v_r, and vertical velocity component, v_z, for angle $\alpha = 120°$.

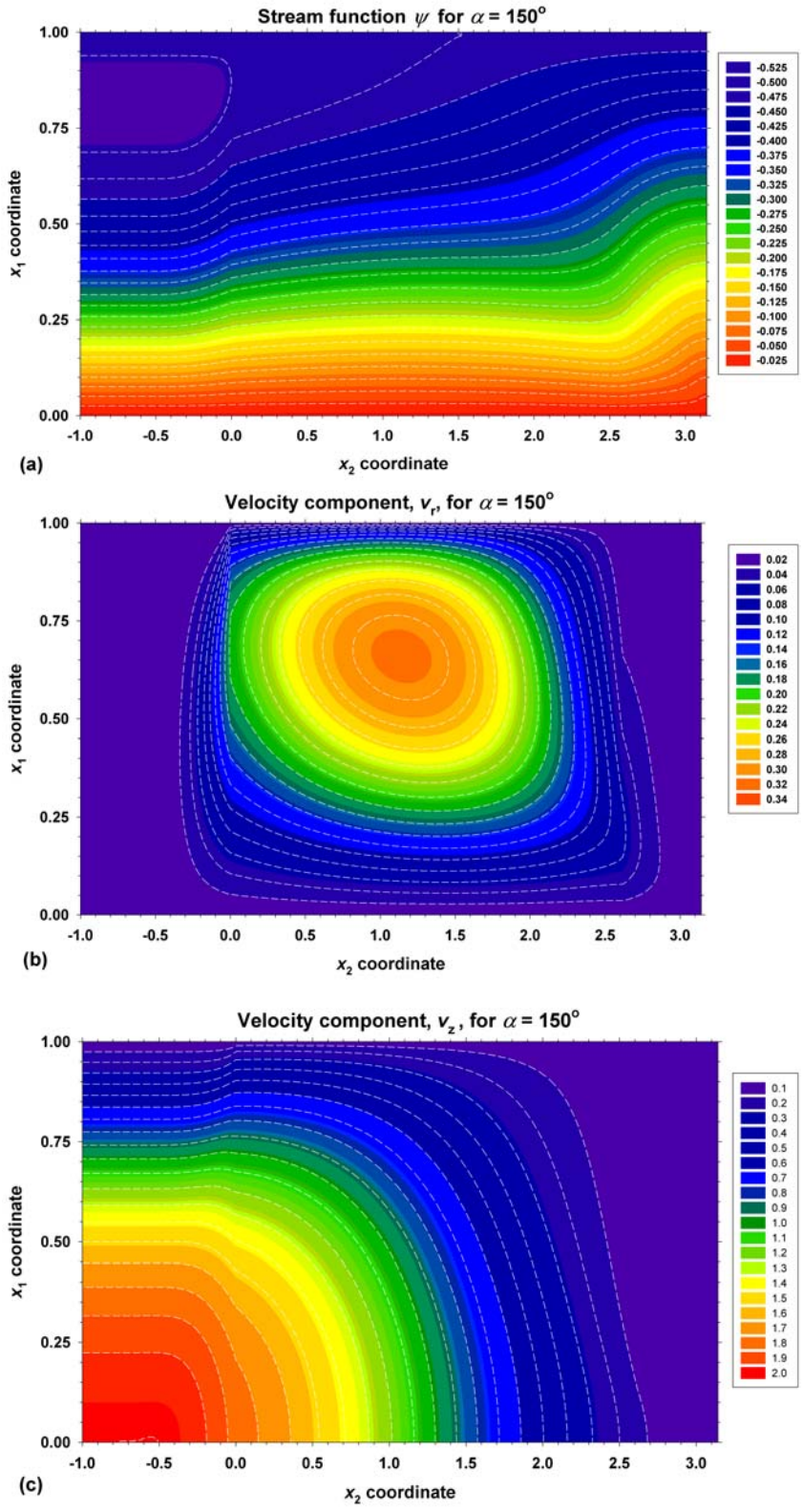

Fig. 7. Calculated (a) stream function, ψ, (b) radial velocity component, v_r, and vertical velocity component, v_z, for angle $\alpha = 150°$.

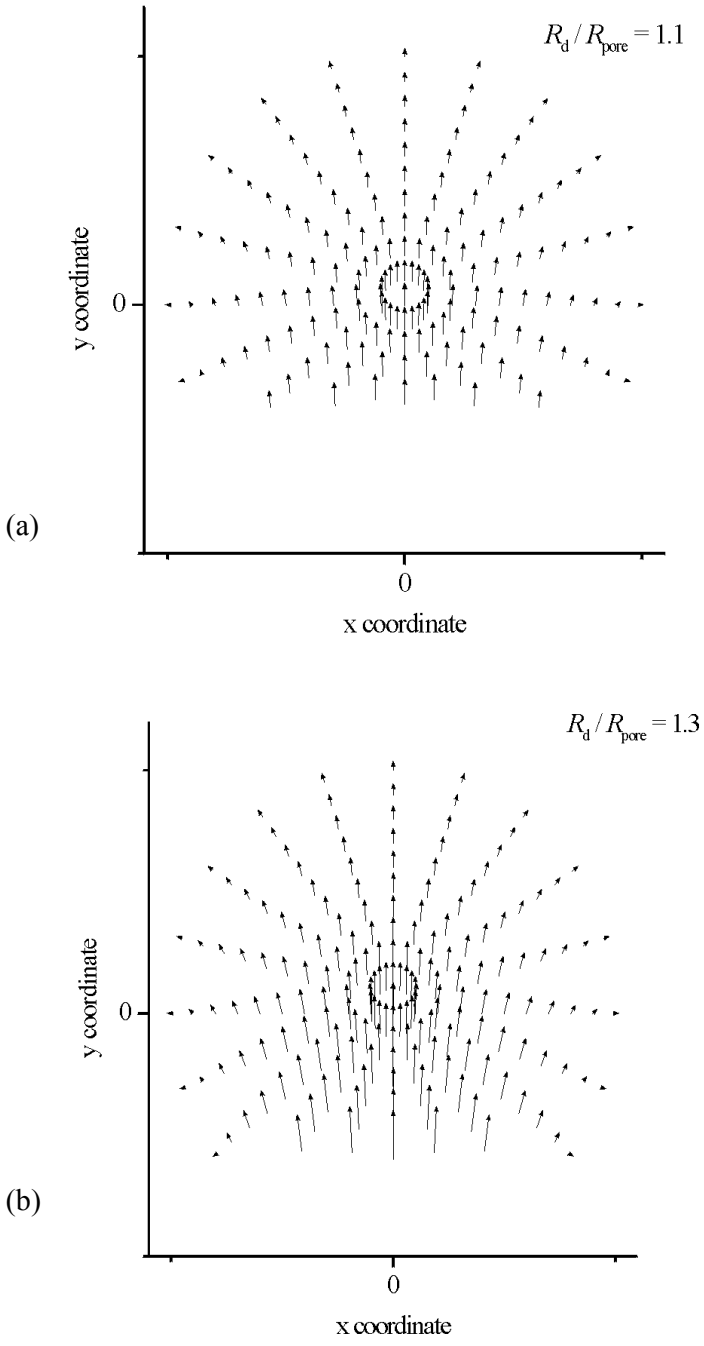

Fig. 8. Distribution of the vector of the velocity in the drop at different values for the ratio R_d / R_{pore}: (a) 1.1 and (b) 1.3.

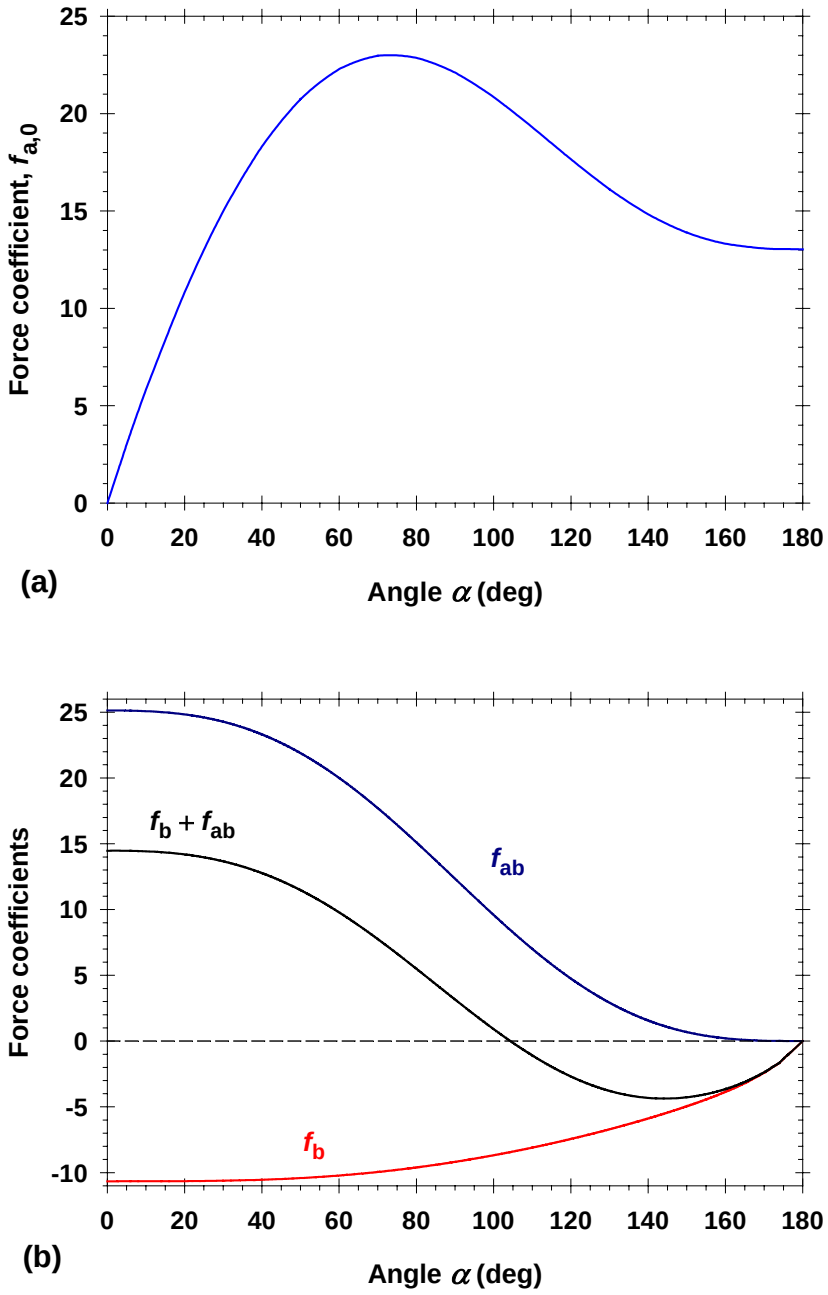

Fig. 9. (a) Force coefficient f_a, and (b) force coefficients f_b and f_{ab}, plotted vs. the angle α.